Hindawi
Mediators of Inflammation
Volume 2023, Article ID 2547588, 11 pages
https://doi.org/10.1155/2023/2547588

Research Article

Dihydromyricetin Inhibits M1 Macrophage Polarization in Atherosclerosis by Modulating miR-9-Mediated SIRT1/NF-κB Signaling Pathway

Zhousheng Yang,[1] **Tianyu Li**,[1,2,3] **Chunyan Wang**,[1,2,3] **Mingyu Meng**,[1] **Shenglan Tan**,[1,2,3] **and Lei Chen**[1,2,3]

[1]*Department of Pharmacy, The People's Hospital of Guangxi Zhuang Autonomous Region, Guangxi Academy of Medical Sciences, Nanning 530021, China*
[2]*Department of Pharmacy, The Second Xiangya Hospital, Central South University, Changsha, China 410011*
[3]*Institute of Clinical Pharmacy, Central South University, Changsha, China 410011*

Correspondence should be addressed to Shenglan Tan; sltan@csu.edu.cn and Lei Chen; mikelei@csu.edu.cn

Received 11 November 2022; Revised 5 April 2023; Accepted 21 April 2023; Published 17 May 2023

Academic Editor: Agnieszka Dobrzyn

Copyright © 2023 Zhousheng Yang et al. This is an open access article distributed under the Creative Commons Attribution License, which permits unrestricted use, distribution, and reproduction in any medium, provided the original work is properly cited.

Dihydromyricetin (DMY), a natural flavonoid compound extracted from the stems and leaves of *Ampelopsis grossedentata*, has been found as a potential therapeutic chemical for treating atherosclerosis. This study explores the underlying mechanism of DMY repressing M1 macrophage polarization in atherosclerosis. We showed that DMY treatment markedly decreased M1 macrophage markers (e.g., Tnf-α and IL-1β) and p65-positive macrophage numbers in the vessel wall of Apoe-deficient ($Apoe^{-/-}$) mice. Overexpression of miR-9 or knockdown of SIRT1 in macrophages reversed the effect of DMY on M1 macrophage polarization. The data we presented in the study indicate that the miR-9-mediated SIRT1/NF-κB pathway plays a pivotal role in M1 macrophage polarization and is one of the molecular mechanisms underlying the anti-atherosclerosis effects of DMY. We provide new solid evidence that DMY may be explored as a potential therapeutic adjuvant for treating atherosclerosis.

1. Introduction

Cardiovascular diseases (CVDs) are the leading cause of mortality worldwide, responsible for one-third of all-cause deaths [1, 2]. The accumulative formation of unstable atherosclerosis plaque in the vessel wall has been recognized as a hallmark in the progress of cardiovascular diseases [3, 4]. Enormous evidence from clinical trials and fundamental researches has demonstrated that atherosclerosis is a lipid-driven chronic inflammatory disease [5–7]. Macrophages, one of the most important immune cells in inflammation, are divided into two subtypes based on their biological functions [8]. One phenotype is M1-like macrophages (classically activated), which secrete inflammatory cytokines (e.g., TNF-α and IL-1β) and promote inflammation. The other one is M2-like macrophages (alternatively activated), which produce anti-inflammatory cytokines (e.g., IL-10 and Arg1) and repair injured tissues. Abnormal activation and infiltration of macrophages in the vessel wall have been identified as a crucial character of unstable plaque. More specifically, increased M1 macrophages with decreased M2 macrophages in the lesion aggravate the vascular inflammation and eventually accelerate atherosclerosis [9, 10].

Dihydromyricetin (DMY), a natural flavonoid compound extracted from the stems and leaves of *Ampelopsis grossedentata*, has been reported to exert anti-inflammatory activities in various diseases [11, 12]. For instance, DMY declines IL-1β and TNF-α levels in the LPS-treated rats' plasma via inhibiting oxidative stress [13]. DMY was also found to inhibit systemic inflammation and prevent infiltration of inflammatory cells in the joints, resulting in relief of synovitis in rheumatoid arthritis [14, 15]. Most recently, Zhou et al. [16] reported that in an exhaustive exercise- (EE-) induced hepatic inflammatory

injury animal model, DMY suppressed hepatic inflammation by orchestrating macrophage polarization. In agreement with these findings, we also observed that DMY decreased the expression of M1 macrophage markers (e.g., Tnf-α and IL-1β) and macrophage accumulation in the vessel wall of *Apoe*$^{-/-}$ mice [17]. However, the underlying mechanisms about how DMY regulates macrophage polarization and alleviates vascular inflammation are largely unknown.

MicroRNAs (miRNAs), a class of small noncoding RNA, have been recognized as potent regulators of various pathological and physiological processes by binding to the 3′UTR of target mRNA [18, 19]. Recently, multiple studies have indicated that miR-9, a highly expressed miRNA in M1 macrophage, plays an essential role in promoting M1 polarization by targeting SIRT1/NF-κB signal pathway activation [20, 21]. In this study, we found that DMY downregulated miR-9 and upregulated its target gene SIRT1 expression both in vivo and in vitro. We identified the role of the miR-9/SIRT1/NF-κB signaling pathway on the antiatherosclerosis effect of DMY, which may, through regulating macrophage polarization and subsequently alleviating vascular inflammation. This study provides new evidence that DMY may emerge as a potential therapeutic adjuvant in treating atherosclerosis.

2. Materials and Methods

2.1. Animal Protocol. All animal procedures were approved by the Institutional Animal Care and Use Committee of Second Xiangya Hospital, Central South University. *Apoe*$^{-/-}$ mice and C57BL/6J mice of 8~12 weeks old were purchased from the Beijing Vital River Laboratory Animal Technology Co. and were fed on a chow diet or a high cholesteric diet (HCD) (D12108C, Research Diets, USA) for 12 weeks. *Apoe*$^{-/-}$ mice were administered daily with DMY (500 mg/kg; D101549, Aladdin; $n = 8$) or the solvent of 0.05% CMC-Na ($n = 10$) via intragastric gavage. The liver, aorta, and peripheral blood mononuclear cells (PBMC) were harvested after 12 weeks. Aortic roots were embedded in an optimal cutting temperature (OCT) compound and stored at -80°C.

2.2. Immunofluorescent Staining. The detail of immunofluorescent staining was described in our previous study [17]. Briefly, the OCT-embedded aorta root was cut into sections at 6 μm using a Lab-Tek tissue processor Leica CM1950. Sections were incubated with anti-Mac-2 (1 : 100, #CL8942AP, Cedarlane) and anti-p65 (1 : 200 dilution, Thermo Fisher Scientific) at 4°C overnight, followed by being stained with Alexa Flour 555 (1 : 300, #A21434, Invitrogen) or 488 (1 : 300, #A11034, Invitrogen) for 1 hour at room temperature. DAPI (#P36935, Invitrogen) was used to label the nuclei. All images were collected by confocal laser scanning microscopy (Nikon, Japan).

2.3. Primary Macrophage Culture, Stimulation, and Transfection. Bone marrow-derived macrophages (BMDMs) were extracted from 12-week-old C57 BL/6J mice. BMDMs were cultured in DMEM medium containing 10% FBS and 10 ng/ml Recombinant Mouse M-CSF Protein (416-ML, R&D), followed by treatment with DMY (50, 100 μmol/L) or control vehicle for one hour, then stimulated with 100 ng/ml LPS (Cat# L2880, Sigma-Aldrich) and 20 ng/ml INF-γ (IF005, Sigma-Aldrich) for 24 hours. Lipofectamine 3000 transfection reagent (L3000008, Invitrogen) was used for miRNA (miR10000142-1-5, miR20000142-1-5, RiboBio) and siRNA (AM16708, Thermo Fisher Scientific) transfection according to the manufacturers' instructions.

2.4. Real-Time qPCR. Total RNA was isolated by TRIzol reagent (15596018, Invitrogen) from the homogenized liver, aorta, and BMDMs. The PrimeScript RT reagent kit (RR047A, Takara) was used to generate cDNA, and the TB Green Premix EX Tag kit (RR820A, Takara) was used for real-time qPCR with the Real-time PCR system (Roche) following the manufacturer's instructions. Specific primers, including miR-9 and U6 (MQPS0000002-1-100), were purchased from RiboBio (Guangzhou, China). Primers' information is listed as follows: β-actin (forward: 5′-GAAATC GTGCGTGACATCAAAG-3′, reverse: 5′-TGTAGTTTCAT GGATGCCACAG-3′); IL-1β (forward: 5′-GCAACTGTT CCTGAACTCAACT-3′, reverse: 5′-ATCTTTTGGGGTCC GTCAACT-3′); IL-6 (forward: 5′-TAGTCCTTCCTACC CCAATTTCC-3′, reverse: 5′-TTGGTCCTTAGCCACT CCTTC-3′); Tnf-α (forward: 5′-CCCTCACACTCAGATC ATCTTCT-3′, reverse: 5′-GCTACGACGTGGGCTACAG-3′); Nos2 (forward: 5′-GTTCTCAGCCCAACAATACAA GA-3′, reverse: 5′-GTGGACGGGTCGATGTCAC-3′); IL-10 (forward: 5′-GCTCTTACTGACTGGCATGAG-3′, reverse: 5′-CGCAGCTCTAGGAGCATGTG-3′); Arg1 (forward: 5′-GTGGAAACTTGCATGGACAAC-3′, reverse: 5′-AATCCTGGCACATCGGGAATC-3′); and SIRT1 (forward: 5′-GACGCTGTGGCAGATTGTTA-3′, reverse: 5′-AAACATGGCTTGAGGGTCTG-3′).

2.5. Western Blot. Protein samples were extracted and measured using a BCA kit (Beyontime, Jiangsu, China). Target protein (20 μg of each sample) was separated by 10% SDS-PAGE gels and then transferred onto 0.45 μm polyvinylidene fluoride (PVDF) membranes (Millipore, Billerica, MA, USA) and followed by incubation with 5% fat-free milk in TBST for 90 min at RT and subsequently interacted with corresponding antibodies as follows: p-p65 and SIRT1 (1 : 1000, Abcam, USA), IkBα (1 : 1000, Cell Signaling Technology, USA), and β-actin (1 : 5000, Sigma, USA) at 4°C overnight. The images were captured using the Bio-Rad Chemi Doc XRS+ Imaging System (Bio-Rad Biosciences, USA).

2.6. Statistical Analysis. All data were analyzed using SPSS 26.0 statistical software (IBM Corp., NY, USA), and GraphPad Prism 8.0 (GraphPad Software, CA, USA) was used for data present in the study. Unpaired two-tailed Student's *t*-test was used to calculate statistical significance between two groups for normally distributed continuous variables. One-way

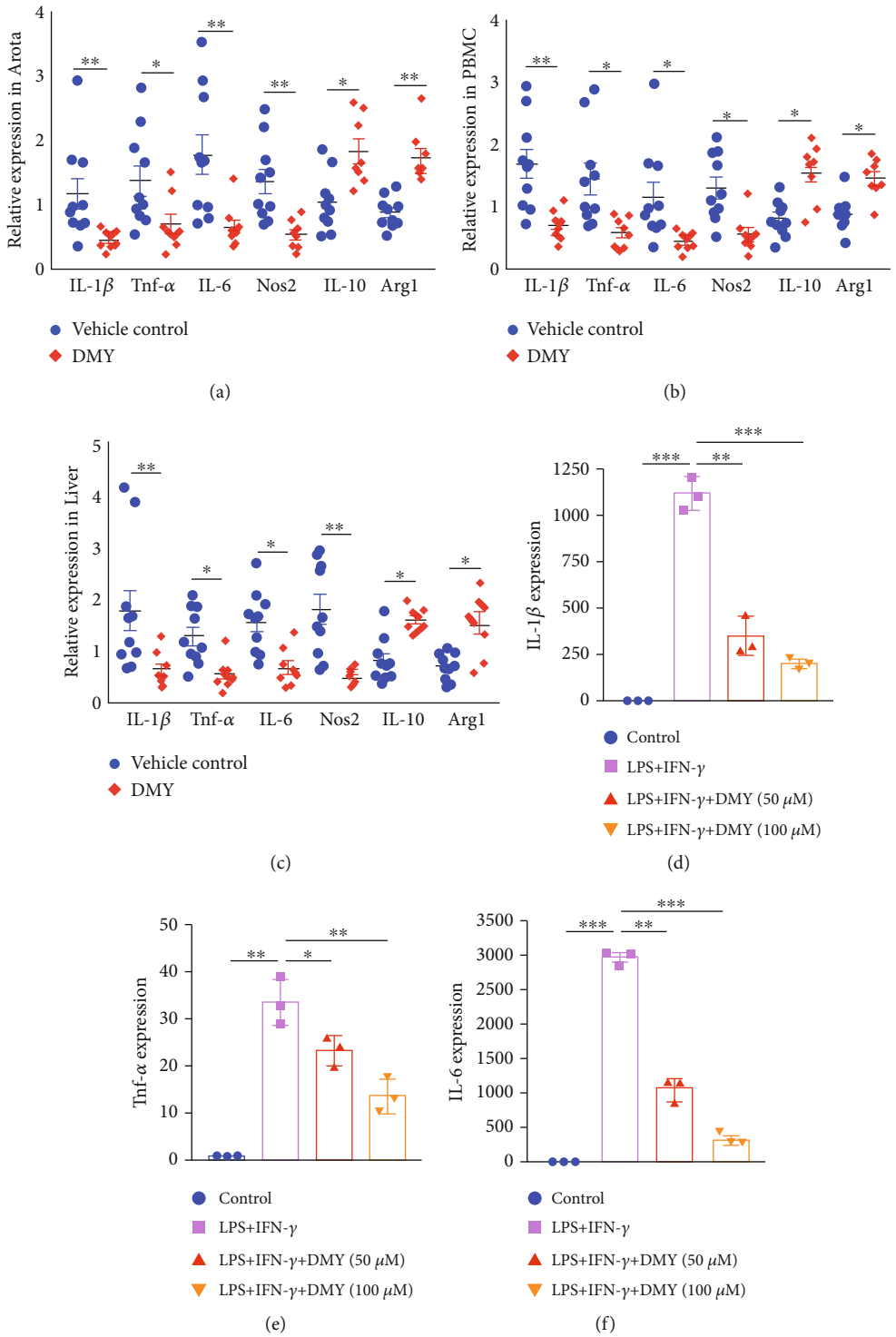

Figure 1: Continued.

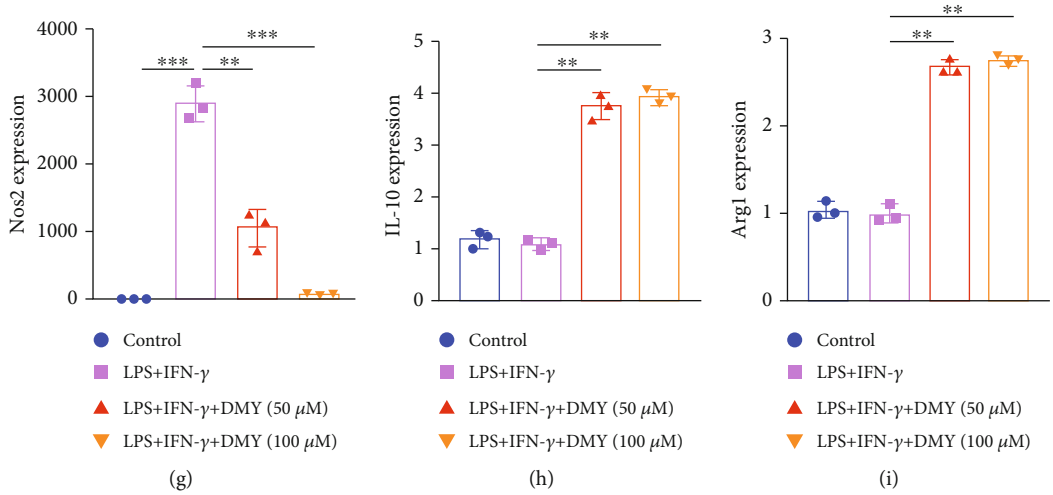

FIGURE 1: (a–c) qPCR analysis of the expression of M1/M2 markers in the tissues between the vehicle control ($n = 10$) and DMY ($n = 8$) groups. (d–i) qPCR verification M1/M2 marker expression in LPS-induced BMDMs with/without DMY treatment ($n = 3$). $^{*}P < 0.05$, $^{**}P < 0.01$, and $^{***}P < 0.001$.

analysis of variance (ANOVA) was utilized for multiple group comparison. Nonparametric Mann–Whitney U test or Kruskal-Wallis test was used for data without normal distribution. All data were expressed as mean ± SEM, and $^{*}P < 0.05$, $^{**}P < 0.01$, and $^{***}P < 0.001$ were considered significant for all tests.

3. Results

3.1. DMY Decreases Expression of M1 Markers and Increases Expression of M2 Markers in Apoe$^{-/-}$ Mice and LPS-Stimulated BMDMs. To investigate whether macrophage polarization is a potential antiatherosclerosis target of DMY, we performed several experiments with the tissues of the aorta, PBMC, and liver from the *Apoe*$^{-/-}$ mice harvested in our previous study [17]. As shown in Figures 1(a)–1(c), compared with vehicle-treated *Apoe*$^{-/-}$ mice, M1 markers' expressions (IL-1β, Tnf-α, IL-6, and Nos2) in the tissues were downregulated and expressions of M2 markers (IL-10 and Arg1) were upregulated in the DMY-treated *Apoe*$^{-/-}$ mice. In line with the in vivo data, qPCR showed that expressions of M1 markers dramatically declined in LPS-stimulated BMDMs with the DMY treatment in a dose-dependent manner (Figures 1(d)–1(g)). Interestingly, elevated M2 marker expressions in the BMDMs with DMY treatment were not significantly different between the high concentration and low concentration of the DMY group (Figures 1(h) and 1(i)). Taken together, our in vivo and in vitro data demonstrate that DMY inhibits M1 macrophage polarization and promotes M2 macrophage polarization in atherosclerosis.

3.2. DMY Suppresses M1 Macrophage Polarization via miR-9 in BMDMs. Numerous studies have indicated that miR-9 plays a crucial role in macrophage polarization in inflammatory diseases [22, 23]. Therefore, we next explored whether miR-9 was associated with DMY's antiatherosclerosis effect. We investigated the expression of miR-9 and found that miR-9 was decreased in the aorta, PBMC, and liver of *Apoe*$^{-/-}$ mice after intragastric gavage with DMY (Figure 2(a)). Consistent with the in vivo data, miR-9 expression was significantly repressed by DMY treatment in the LPS-stimulated BMDMs (Figure 2(b)). Transfection of miR-9 mimic was used to validate this hypothesis. As we expected, the downregulation of IL-1β, Tnf-α, IL-6, and Nos2 expressions was reversed by miR-9 transfection in the DMY group (Figures 2(c)–2(f)). To our surprise, increased expression of IL-10 and Arg1 in BMDMs with DMY treatment could not be reversed by miR-9 transfection (Figures 2(g) and 2(h)). In summary, these results indicate that overexpression of miR-9 could abrogate the effect of DMY on M1 macrophage polarization but not M2 macrophages.

3.3. miR-9 Mediates the Effect of DMY on M1 Macrophage Polarization by Targeting SIRT1/NF-κB Signaling Pathway in BMDMs. The abnormal activation of the NF-κB signaling pathway is a core factor in M1 macrophage polarization and the pathogenesis of atherosclerosis. The NF-κB signaling pathway has been reported as a potential pharmacological target for DMY [24–26]. As shown in Figure 3(a), we found that DMY diminished Mac2 positive/p-65 positive cell numbers in the aortic sinus lesions of *Apoe*$^{-/-}$ mice. How does DMY affect macrophage polarization and eventually ameliorate atherosclerosis? Recently, Wang et al. [21] revealed that miR-9 promoted M1 macrophage polarization in osteoarthritis progression by targeting SIRT1 and subsequently activating the NF-κB signal pathway. In agreement with Wang et al.'s study, we found that SIRT1 was a direct target of miR-9 in macrophages (Figure 3(b)). Moreover, elevated SIRT1 expression was observed in *Apoe*$^{-/-}$ mice with DMY treatment, which indicated that the miR-9/SIRT1 pathway may contribute to the regulation of DMY on M1 macrophage polarization (Figure 3(c)). Thus, we transfected miR-9 mimic in BMDMs and found that miR-9 transfection

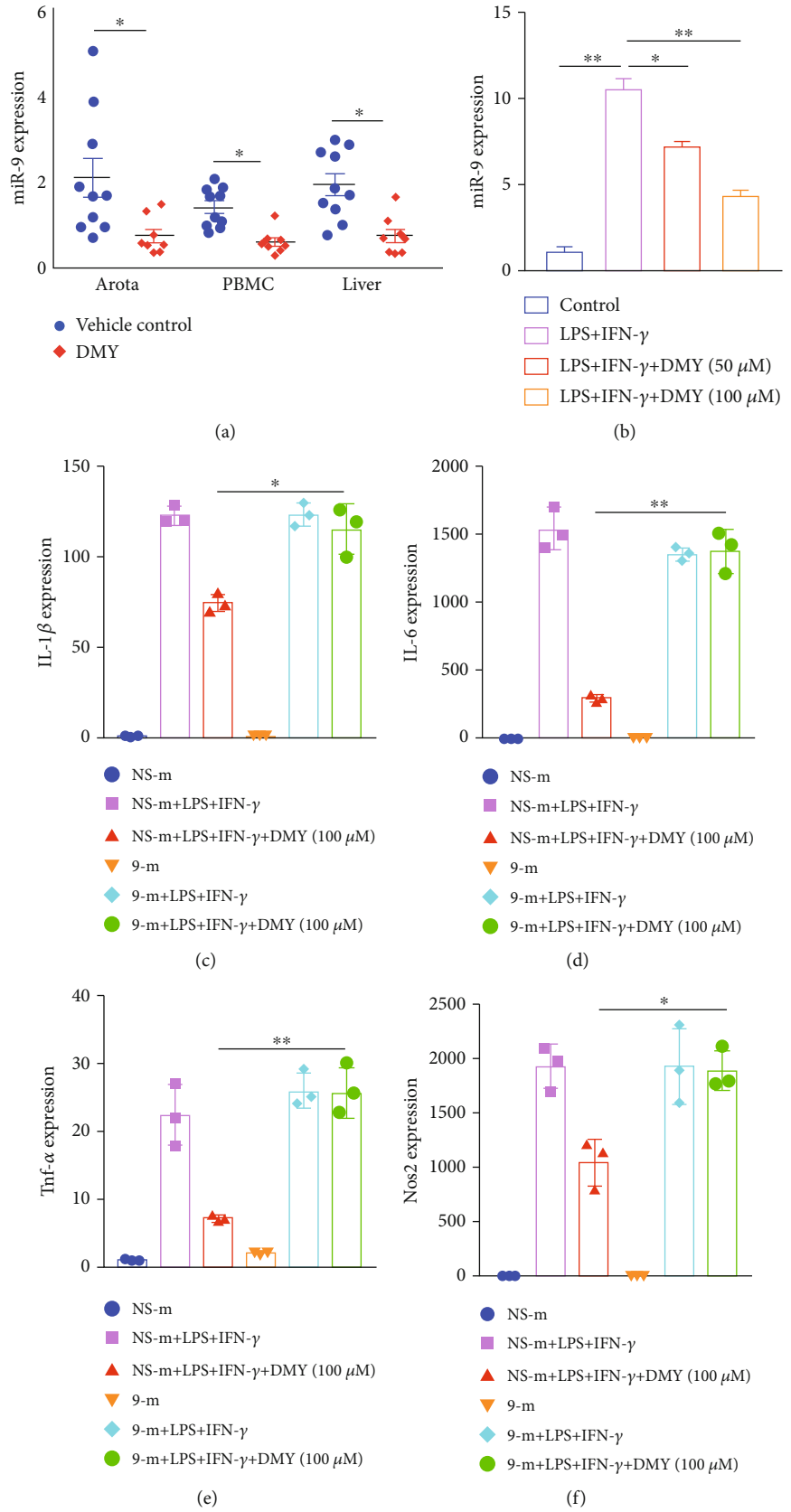

Figure 2: Continued.

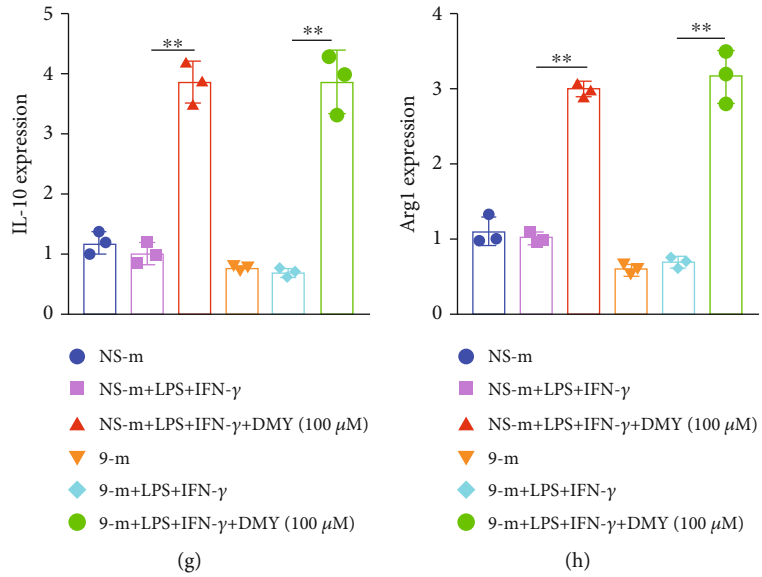

Figure 2: (a) The expression of miR-9 in the vehicle control ($n = 10$) and DMY ($n = 8$) groups. (b) qPCR detection of miR-9 expression in BMDMs in each group ($n = 3$). (c–h) Analysis of M1/M2 markers after mimic Nc and miR-9 transfection in treated BMDMs in each group ($n = 3$). $^{*}P < 0.05$ and $^{**}P < 0.01$.

abolished the increased expression of SIRT1 and inhibited the NF-κB signaling pathway under the treatment of DMY (Figures 3(d)–3(g)). The data mentioned above indicate that DMY suppresses M1 macrophage polarization, probably by targeting the miR-9/SIRT1/NF-κB signaling pathway.

3.4. The Effect of DMY on M1 Macrophage Polarization Depends on the SIRT1/NF-κB Signaling Pathway in BMDMs. To confirm whether SIRT1 was involved in the effect of DMY on M1 macrophage polarization, siRNA was used to knock down the expression of SIRT1 in BMDMs. We found that silence of SIRT1 rescued the decrease of IkBα and p-p65 in BMDMs treated with DMY (Figures 4(a)–4(c)); meanwhile, the declined expressions of M1 markers (IL-1β, Tnf-α, IL-6, and Nos2) in the DMY group were also reversed (Figures 4(d)–4(g)). These results reveal that SIRT1 is the crucial factor contributing to the effect of DMY on M1 macrophage polarization by modulating the NF-κB signaling pathway.

4. Discussion

Accumulating clinical and experimental studies have demonstrated that traditional Chinese herbal medicine is a promising therapy for cardiovascular diseases [27, 28]. Here, we provided evidence that DMY relieved vascular inflammation and repressed M1 macrophage polarization in atherosclerosis through modulating the miR-9/SIRT1/NF-κB signal pathway. Overexpression of miR-9 or knockdown of SIRT1 expression in macrophage could both reverse the effect of DMY on M1 macrophage polarization. The data we presented above indicate that the miR-9-mediated SIRT1/NF-κB pathway plays a pivotal role in M1 macrophage polarization and is one of the molecular mechanisms underlying the antiatherosclerosis effects of DMY.

Macrophages are involved in all stages of atherosclerosis, from lesion initiation to rupture of advanced lesions. More specifically, M1 and M2 macrophages are recruited to the intima at an early stage to eliminate accumulated lipids and repair injured tissue. In the advanced stage, cumulative M1 macrophages and decreased M2 macrophages appear in the lesion, leading to the formation of a necrotic core which may result in a cardiovascular event [29, 30]. Targeting macrophage polarization is considered one of the most promising therapeutic strategies for atherosclerosis [31]. Recently, Zhou et al. [16] found that DMY-encapsulated liposomes efficiently inhibited exercise-induced liver inflammation by targeting hepatic macrophages, repressing M1 macrophage polarization, and promoting M2 macrophage polarization. Our previous study also reported that DMY inhibited macrophage accumulation in the aortic sinus lesions and liver of *Apoe*$^{-/-}$ mice [17]. In the present study, decreased expressions of M1 markers and increased expressions of M2 markers in the circulating monocytes, livers, and aorta were observed in DMY-treated *Apoe*$^{-/-}$ mice (Figures 1 and 3(a)). Our data suggested that M1/M2 polarization may be an essential target for DMY to alleviate vascular inflammation and eventually ameliorate atherosclerosis.

How does DMY regulate M1/M2 polarization? Numerous studies have demonstrated that highly expressed miR-9 in macrophage induced by pathological stimulus (e.g., LPS) during the inflammatory response is associated with M1 polarization [32, 33]. Tong et al. [20] showed that head and neck squamous cell carcinoma- (HNSCC-) derived exosomal miR-9 could induce M1 macrophage polarization. In support, another study [34] found that lipotoxic hepatocyte-derived extracellular vesicle- (EV-) encapsulated miR-9-5p markedly activated hepatic macrophage M1 polarization both in vivo and in vitro. These researches indicate that miR-9 secreted and delivered from macrophages or other cell types can induce M1 macrophage polarization. Thus, we hypothesized that

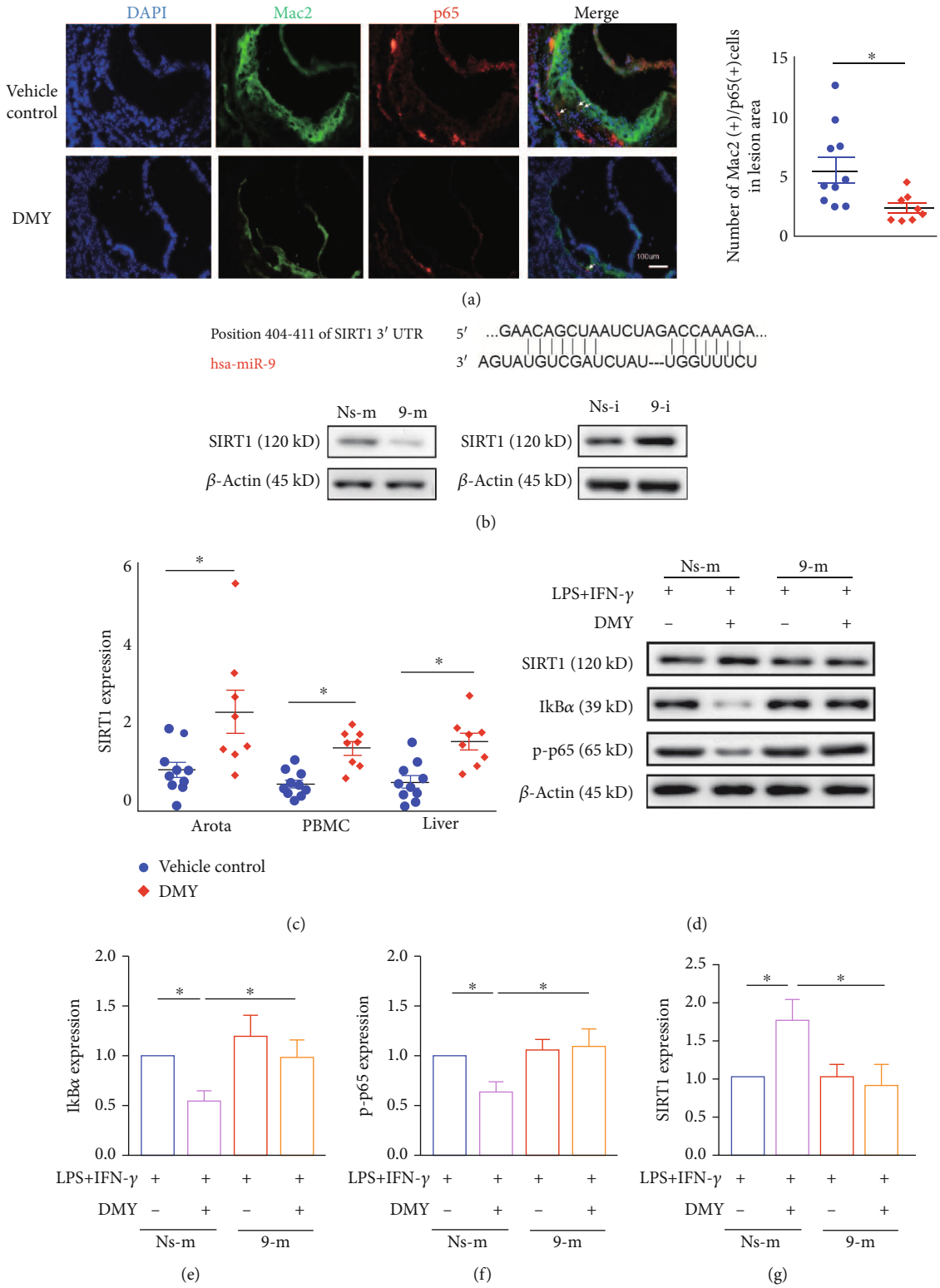

Figure 3: (a) Representative images are shown p65 colocalized with Mac2 in the aortic sinus lesions of the vehicle control and DMY groups. Scale bar, 100 μm. (b) The binding site between miR-9 and SIRT1 was predicted by the TargetScan database. (c) qPCR examines the expression of SIRT1 in the tissues. (d–g) Western blot analysis of NF-κB signaling pathway in BMDMs in each group ($n = 3$). $^*P < 0.05$.

miR-9 was a potential target of DMY in macrophages, which mediated the effect of DMY on macrophage polarization. As we expected, downregulation of miR-9 expression was observed in DMY-treated *Apoe*$^{-/-}$ mice and BMDMs (Figures 2(a) and 2(b)). More critically, overexpression of miR-9 by miR-9 mimic in BMDMs entirely blocked the inhibition effect of DMY on M1 macrophage polarization (Figures 2(c)–2(f)). Surprisingly, DMY-induced increased

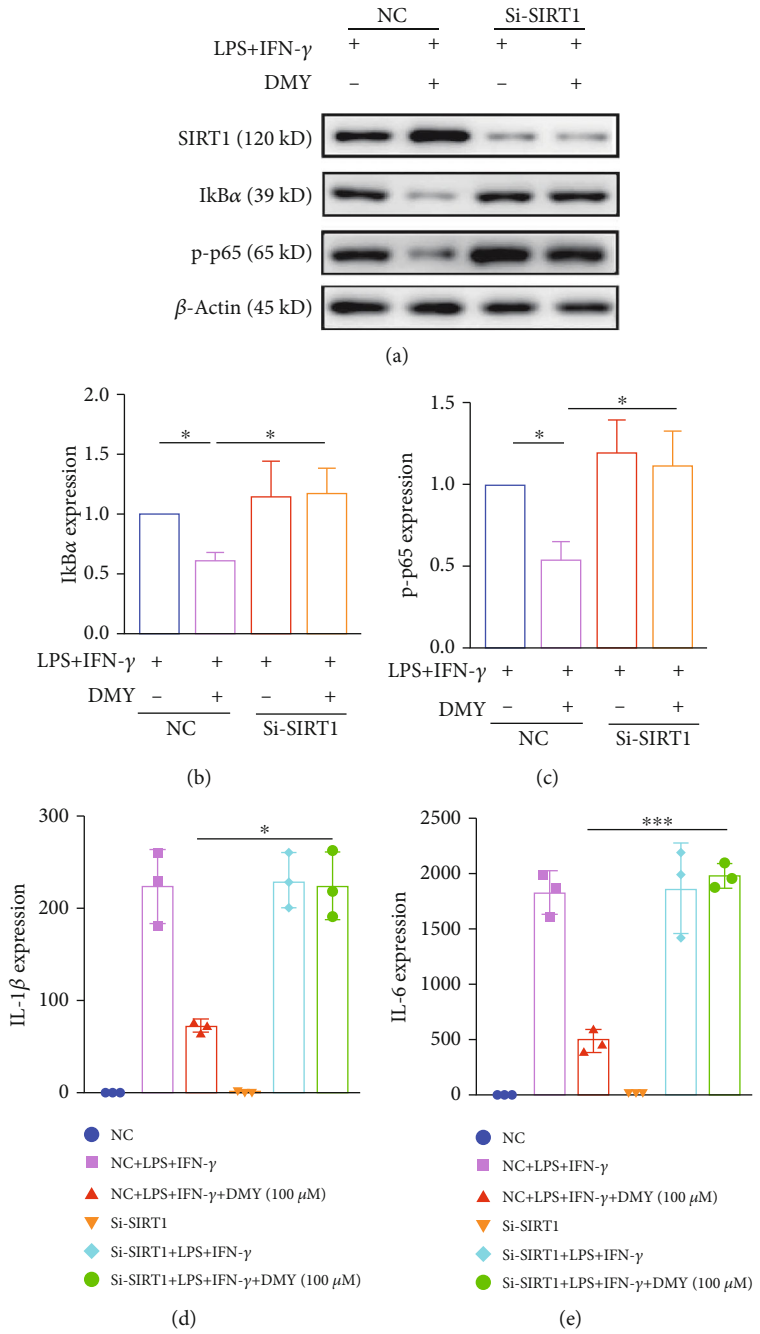

Figure 4: Continued.

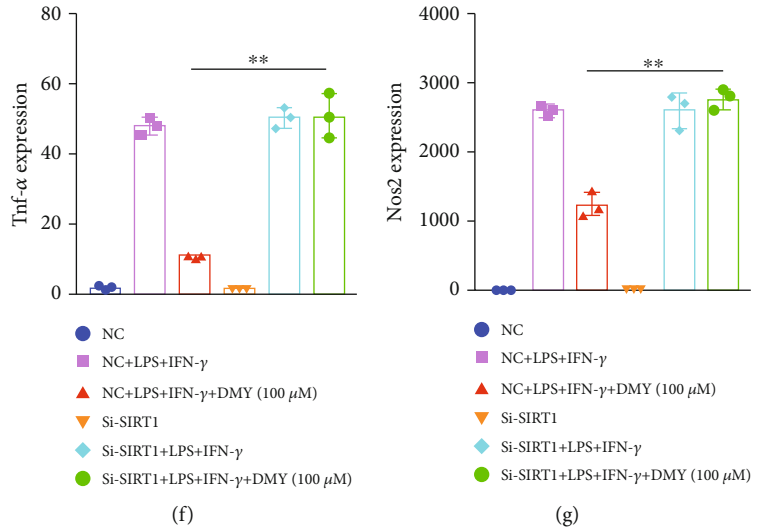

Figure 4: (a–c) Western blot detects SIRT1 and NF-κB signaling pathway in each group ($n = 3$). (d–g) qPCR examines the expression of M1 markers in BMDMs in each group ($n = 3$). $^{*}P < 0.05$, $^{**}P < 0.01$, and $^{***}P < 0.001$.

expressions of M2 markers in macrophage cannot be abrogated by miR-9 overexpression (Figures 2(g) and 2(h)). Our data indicated that miR-9 mediated the regulation of DMY on M1 macrophage polarization but not M2 macrophage polarization. The underlying molecular mechanisms of DMY on M2 macrophage polarization require further investigation.

Impaired expression of SIRT1 promotes p65 nucleus translocation in macrophages, resulting in the phenotype switching to M1 [35]. An increasing number of data showed that traditional Chinese herbs, including DMY, alleviated inflammation by modulating M1/M2 polarization in a SIRT1/NF-κB pathway-dependent manner. Zeng et al. [36] recently reported that DMY treatment increased hepatic SIRT1 expression and subsequently repressed the NF-κB signal pathway in nonalcoholic steatohepatitis (NASH) mice. Consistent with Zeng et al.'s finding, we found that DMY elevated SIRT1 expression in *Apoe*$^{-/-}$ mice and BMDMs (Figures 3(c) and 3(d)). More importantly, overexpression of miR-9 repressed the increased expression of SIRT1 in DMY-treated BMDMs (Figure 3(d)). Knockdown of SIRT1 in macrophages promoted NF-κB pathway activation and abrogated the suppression of DMY on M1 macrophage polarization (Figure 4). Taken together, we hypothesized that DMY modulated SIRT1 expression by decreasing the expression of miR-9, which can inhibit NF-κB pathway activation and M1 macrophage polarization. Of note, Zhou et al.'s [16] finding revealed that SIRT3 was the critical target for DMY-encapsulated liposomes to orchestrate M1/M2 macrophage polarization and improve exhaustive exercise-induced hepatic inflammation. However, our study did not investigate if SIRT3 played a role in the antiatherosclerosis effect of DMY, which will be examined in future studies.

In this study, DMY alleviated vascular inflammation by orchestrating M1/M2 macrophage polarization. Zeng et al. [37] also revealed that DMY facilitates macrophage cholesterol efflux and prevents foam cell formation in an LXRα-ABCA1/ABCG1-dependent manner. Moreover, we [17] and Liu et al. [38] confirmed that DMY increased endothelial nitric oxide

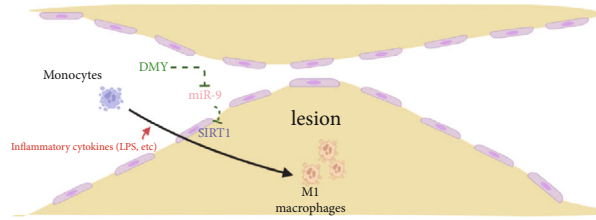

Figure 5: Scheme of miR-9 mediates the inhibition of DMY on M1 macrophage polarization in atherosclerosis.

production, improved lipid profiles, downregulated hepatic inflammation, and inhibited atherosclerosis. In addition, DMY could modulate gut microbiota to either improve DSS-induced colitis or exert an antiobesity effect [39, 40]. These previous findings indicate that gut microbiota is a potential target for DMY in treating atherosclerosis. Collectively, DMY exerts antiatherosclerosis activities by targeting multiple cell types, tissues, and gut microbiota involved in the pathological process of atherogenesis. Herein, in the present data, we highlight that orchestrating M1/M2 polarization may be an essential target for DMY to alleviate vascular inflammation and ameliorate atherosclerosis. Furthermore, the miR-9-mediated SIRT1/NF-κB pathway is a crucial target for DMY to inhibit M1 macrophage polarization.

There are several limitations in our research. Firstly, our data from the in vivo samples (aorta, PBMC, and liver) was based on mixed cell populations, and macrophage-specific miR-9 knockout/in mice are needed to validate our hypothesis further. Secondly, miR-9 mediated the effect of DMY on M1 macrophage polarization but not M2 macrophage polarization, which indicates that other regulation mechanisms may contribute to the impact of DMY on orchestrating macrophage polarization.

5. Conclusion

In summary, our data demonstrate that miR-9 contributes to the inhibition effect of DMY on M1 macrophage

polarization, at least in part, by targeting SIRT1 and activating the NF-κB pathway in atherosclerosis (Figure 5). Our findings shed new insights on how DMY regulates macrophage activation and provides solid evidence that DMY may be explored as a potential therapeutic adjuvant in treating atherosclerosis.

Data Availability

The datasets used and/or analyzed during the current study are available from the corresponding authors upon reasonable request.

Conflicts of Interest

The authors declare no conflicts of interest.

Authors' Contributions

Lei Chen and Shenglan Tan designed the research. Lei Chen and Zhousheng Yang performed the research. Shenglan Tan and Chunyan Wang analyzed the data and performed the statistical analysis. Tianyu Li and Mingyu Meng wrote the paper.

Acknowledgments

This work was supported by the National Natural Science Foundation of China (no. 81703818), the GuangXi Province Natural Science Foundation of China (no. 2021JJA141286), the Hunan Province Natural Science Foundation of China (nos. 2019JJ40430 and 2018JJ3731), the ChangSha Natural Science Foundation of China (no. kq2202391 and no. kq2202394), the Central South University Research Programme of Advanced Interdisciplinary Studies (no. 2023QYJC040), and the Hunan Administration of Traditional Chinese Medicine Grant (no. B2023062).

References

[1] R. C. Hermida, J. J. Crespo, M. Domínguez-Sardiña et al., "Bedtime hypertension treatment improves cardiovascular risk reduction: the Hygia Chronotherapy Trial," *European Heart Journal*, vol. 41, no. 48, pp. 4565–4576, 2020.

[2] D. Fitchett, S. E. Inzucchi, C. P. Cannon et al., "Empagliflozin reduced mortality and hospitalization for heart failure across the spectrum of cardiovascular risk in the EMPA-REG OUTCOME trial," *Circulation*, vol. 139, no. 11, pp. 1384–1395, 2019.

[3] P. Gaede, P. Vedel, N. Larsen, G. V. H. Jensen, H.-H. Parving, and O. Pedersen, "Multifactorial intervention and cardiovascular disease in patients with type 2 diabetes," *The New England Journal of Medicine*, vol. 348, no. 5, pp. 383–393, 2003.

[4] M. Guasch-Ferré, F. B. Hu, M. A. Martínez-González et al., "Olive oil intake and risk of cardiovascular disease and mortality in the PREDIMED study," *BMC Medicine*, vol. 12, no. 1, p. 78, 2014.

[5] P. M. Ridker, B. M. Everett, T. Thuren et al., "Anti-inflammatory therapy with canakinumab for atherosclerotic disease," *The New England Journal of Medicine*, vol. 377, no. 12, pp. 1119–1131, 2017.

[6] A. Haghikia, F. Zimmermann, P. Schumann et al., "Propionate attenuates atherosclerosis by immune-dependent regulation of intestinal cholesterol metabolism," *European Heart Journal*, vol. 43, no. 6, pp. 518–533, 2022.

[7] D. Guo, Z. Zhu, C. Zhong et al., "Prognostic metrics associated with inflammation and atherosclerosis signaling evaluate the burden of adverse clinical outcomes in ischemic stroke patients," *Clinical Chemistry*, vol. 66, no. 11, pp. 1434–1443, 2020.

[8] L.-X. Wang, S.-X. Zhang, H.-J. Wu, X.-L. Rong, and J. Guo, "M2b macrophage polarization and its roles in diseases," *Journal of Leukocyte Biology*, vol. 106, no. 2, pp. 345–358, 2019.

[9] P. M. Ridker, J. G. MacFadyen, T. Thuren et al., "Effect of interleukin-1β inhibition with canakinumab on incident lung cancer in patients with atherosclerosis: exploratory results from a randomised, double-blind, placebo-controlled trial," *Lancet*, vol. 390, no. 10105, pp. 1833–1842, 2017.

[10] P. M. Ridker, B. M. Everett, A. Pradhan et al., "Low-dose methotrexate for the prevention of atherosclerotic events," *The New England Journal of Medicine*, vol. 380, no. 8, pp. 752–762, 2019.

[11] L. Hou, F. Jiang, B. Huang et al., "Dihydromyricetin resists inflammation-induced muscle atrophy via ryanodine receptor-CaMKK-AMPK signal pathway," *Journal of Cellular and Molecular Medicine*, vol. 25, no. 21, pp. 9953–9971, 2021.

[12] T. Xiao, Y. Wei, M. Cui et al., "Effect of dihydromyricetin on SARS-CoV-2 viral replication and pulmonary inflammation and fibrosis," *Phytomedicine*, vol. 91, article 153704, 2021.

[13] J. Peng, J. Zhang, L. Zhang, Y. Tian, Y. Li, and L. Qiao, "Dihydromyricetin improves vascular hyporesponsiveness in experimental sepsis via attenuating the over-excited MaxiK and K channels," *Pharmaceutical Biology*, vol. 56, no. 1, pp. 344–350, 2018.

[14] J. Chu, X. Wang, H. Bi, L. Li, M. Ren, and J. Wang, "Dihydromyricetin relieves rheumatoid arthritis symptoms and suppresses expression of proinflammatory cytokines via the activation of Nrf2 pathway in rheumatoid arthritis model," *International Immunopharmacology*, vol. 59, pp. 174–180, 2018.

[15] J. Wu, K.-J. Fan, Q.-S. Wang, B.-X. Xu, Q. Cai, and T.-Y. Wang, "DMY protects the knee joints of rats with collagen-induced arthritis by inhibition of NF-κB signaling and osteoclastic bone resorption," *Food & Function*, vol. 11, no. 7, pp. 6251–6264, 2020.

[16] X. Zhou, L. Yi, H. Lang et al., "Dihydromyricetin-encapsulated liposomes inhibit exhaustive exercise-induced liver inflammation by orchestrating M1/M2 macrophage polarization," *Frontiers in Pharmacology*, vol. 13, article 887263, 2022.

[17] D. Yang, Z. Yang, L. Chen et al., "Dihydromyricetin increases endothelial nitric oxide production and inhibits atherosclerosis through microRNA-21 in apolipoprotein E-deficient mice," *Journal of Cellular and Molecular Medicine*, vol. 24, no. 10, pp. 5911–5925, 2020.

[18] A. Najm, F.-M. Masson, P. Preuss et al., "MicroRNA-17-5p reduces inflammation and bone erosions in mice with collagen- induced arthritis and directly targets the JAK/STAT pathway in rheumatoid arthritis fibroblast-like synoviocytes," *Arthritis & Rhematology*, vol. 72, no. 12, pp. 2030–2039, 2020.

[19] H. Wang, W. Mehal, L. E. Nagy, and Y. Rotman, "Immunological mechanisms and therapeutic targets of fatty liver diseases," *Cellular & Molecular Immunology*, vol. 18, no. 1, pp. 73–91, 2021.

[20] F. Tong, X. Mao, S. Zhang et al., "HPV + HNSCC-derived exosomal miR-9 induces macrophage M1 polarization and increases tumor radiosensitivity," *Cancer Letters*, vol. 478, pp. 34–44, 2020.

[21] J. Wang, S. Ma, J. Yu et al., "MiR-9-5p promotes M1 cell polarization in osteoarthritis progression by regulating NF-κB and AMPK signaling pathways by targeting SIRT1," *International Immunopharmacology*, vol. 101, no. Part A, article 108207, 2021.

[22] W. Ma, W. Zhang, B. Cui et al., "Functional delivery of lncRNA TUG1 by endothelial progenitor cells derived extracellular vesicles confers anti-inflammatory macrophage polarization in sepsis via impairing miR-9-5p-targeted SIRT1 inhibition," *Cell Death & Disease*, vol. 12, no. 11, p. 1056, 2021.

[23] T. Xin, C. Lu, J. Zhang et al., "Oxidized LDL disrupts metabolism and inhibits macrophage survival by activating a miR-9/Drp1/mitochondrial fission signaling pathway," *Oxidative Medicine and Cellular Longevity*, vol. 2020, Article ID 8848930, 16 pages, 2020.

[24] Y. Zhao, X. Liu, C. Ding, Y. Gu, and W. Liu, "Dihydromyricetin reverses thioacetamide-induced liver fibrosis through inhibiting NF-κB-mediated inflammation and TGF-β1-regulated of PI3K/Akt signaling pathway," *Frontiers in Pharmacology*, vol. 12, article 783886, 2021.

[25] N. Tang, J. Ma, K. S. Wang et al., "Dihydromyricetin suppresses TNF-α-induced NF-κB activation and target gene expression," *Molecular and Cellular Biochemistry*, vol. 422, no. 1-2, pp. 11–20, 2016.

[26] A. I. Matouk, E. M. Awad, N. F. G. El-Tahawy, A. A. K. El-Sheikh, and S. Waz, "Dihydromyricetin alleviates methotrexate-induced hepatotoxicity via suppressing the TLR4/NF-κB pathway and NLRP3 inflammasome/caspase 1 axis," *Biomedicine & Pharmacotherapy*, vol. 155, article 113752, 2022.

[27] P.-P. Hao, F. Jiang, Y.-G. Chen et al., "Traditional Chinese medication for cardiovascular disease," *Nature Reviews Cardiology*, vol. 12, no. 2, pp. 115–122, 2015.

[28] X. Y. Guo, J. Liu, J. Liu et al., "Use of traditional Chinese medicine in Chinese patients with coronary heart disease," *Biomedical and Environmental Sciences*, vol. 26, no. 4, pp. 303–310, 2013.

[29] I. Tabas and K. E. Bornfeldt, "Intracellular and intercellular aspects of macrophage immunometabolism in atherosclerosis," *Circulation Research*, vol. 126, no. 9, pp. 1209–1227, 2020.

[30] T. Josefs, T. J. Barrett, E. J. Brown et al., "Neutrophil extracellular traps promote macrophage inflammation and impair atherosclerosis resolution in diabetic mice," *Insight*, vol. 5, no. 7, 2020.

[31] C. Gao, Q. Huang, C. Liu et al., "Treatment of atherosclerosis by macrophage-biomimetic nanoparticles via targeted pharmacotherapy and sequestration of proinflammatory cytokines," *Nature Communications*, vol. 11, no. 1, p. 2622, 2020.

[32] W. F. Carson, S. E. Salter-Green, M. M. Scola, A. Joshi, K. A. Gallagher, and S. L. Kunkel, "Enhancement of macrophage inflammatory responses by CCL2 is correlated with increased miR-9 expression and downregulation of the ERK1/2 phosphatase Dusp6," *Cellular Immunology*, vol. 314, pp. 63–72, 2017.

[33] L. Lu, S. McCurdy, S. Huang et al., "Time series miRNA-mRNA integrated analysis reveals critical miRNAs and targets in macrophage polarization," *Scientific Reports*, vol. 6, no. 1, article 37446, 2016.

[34] H. Liu, Q. Niu, T. Wang, H. Dong, and C. Bian, "Lipotoxic hepatocytes promote nonalcoholic fatty liver disease progression by delivering microRNA-9-5p and activating macrophages," *International Journal of Biological Sciences*, vol. 17, no. 14, pp. 3745–3759, 2021.

[35] A. Kauppinen, T. Suuronen, J. Ojala, K. Kaarniranta, and A. Salminen, "Antagonistic crosstalk between NF-κB and SIRT1 in the regulation of inflammation and metabolic disorders," *Cellular Signalling*, vol. 25, no. 10, pp. 1939–1948, 2013.

[36] Y. Zeng, Y. Q. Hua, W. Wang, H. Zhang, and X. L. Xu, "Modulation of SIRT1-mediated signaling cascades in the liver contributes to the amelioration of nonalcoholic steatohepatitis in high fat fed middle-aged LDL receptor knockout mice by dihydromyricetin," *Biochemical Pharmacology*, vol. 175, article 113927, 2020.

[37] Y. Zeng, Y. Peng, K. Tang et al., "Dihydromyricetin ameliorates foam cell formation via LXRα- ABCA1/ABCG1-dependent cholesterol efflux in macrophages," *Biomedicine & Pharmacotherapy*, vol. 101, pp. 543–552, 2018.

[38] T. T. Liu, Y. Zeng, K. Tang, X. Chen, W. Zhang, and X. L. Xu, "Dihydromyricetin ameliorates atherosclerosis in LDL receptor deficient mice," *Atherosclerosis*, vol. 262, pp. 39–50, 2017.

[39] S. Dong, M. Zhu, K. Wang et al., "Dihydromyricetin improves DSS-induced colitis in mice via modulation of fecal- bacteria-related bile acid metabolism," *Pharmacological Research*, vol. 171, article 105767, 2021.

[40] Y. Song, L. Sun, P. Ma, L. Xu, and P. Xiao, "Dihydromyricetin prevents obesity via regulating bile acid metabolism associated with the farnesoid X receptor in ob/ob mice," *Food & Function*, vol. 13, no. 5, pp. 2491–2503, 2022.